

Online Supporting Figures and Tables for

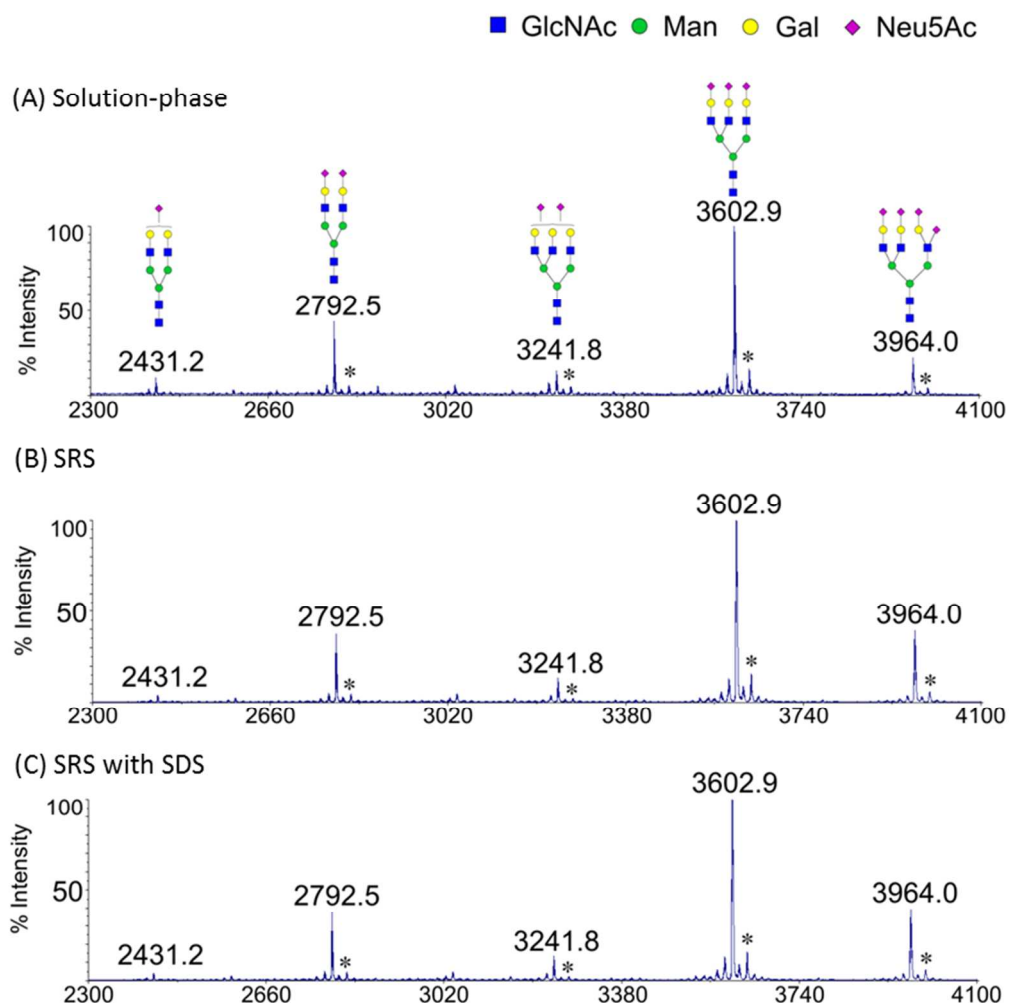
Universal Solid-phase Reversible Sample-Prep for Concurrent Proteome and N-glycome Characterization

Hui Zhou, Samantha Morley, Stephen Kostel, Michael R. Freeman, Vivek Joshi, David Brewster, Richard S. Lee

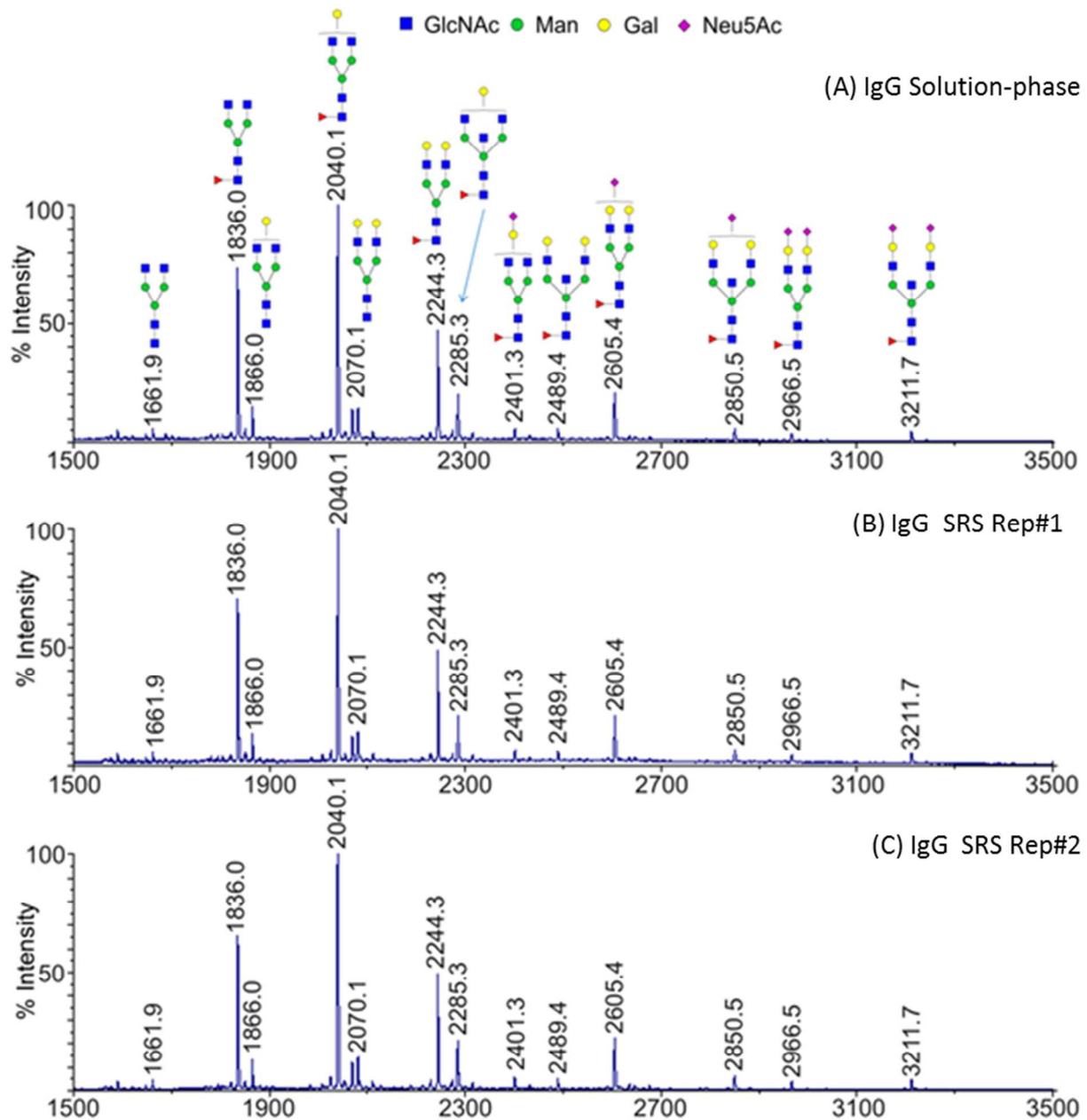
Correspondence should be addressed to:

Richard S. Lee, MD
Boston Children's Hospital
Department of Urology
300 Longwood Avenue
Hunnewell 390
Boston, MA 02115
Richard.Lee@childrens.harvard.edu
617-355-3348 (Phone)
617-730-0474 (fax)

- Supporting Figure 1: Comparison of MALDI-MS of permethylated N-glycans of bovine fetuin by different Sample-Prep Strategies.
- Supporting Figure 2: Comparison of MALDI-MS of permethylated N-glycans of human serum IgG by different Sample-Prep Strategies.
- Supporting Figure 3: Comparison of MALDI-MS of permethylated N-glycans from two different murine kidneys.
- Supporting Figure 4: Comparison of MALDI-MS of permethylated N-glycans from two different murine bladders.
- Supporting Figure 5: MALDI-MS of permethylated N-glycans from human urine specimen.
- Supporting Figure 6: Replicate LC-MS/MS total ion chromatographs (TIC) of fetuin tryptic peptides obtained using the SRS method.
- Supporting Figure 7: Proteomic and glycoproteomic comparison of technical or biologic replicates of various biologic samples processed by SRS.
- Supporting Figure 8: Comparison of MALDI-MS of permethylated N-glycans from DU145Ctrl and DU145KD.
- Supporting Table 1: The identified N-glycans from two different murine kidneys processed and analyzed using SRS and MALDI-MS.
- Supporting Table 2: The identified N-glycans from two different murine bladder tissue samples processed and analyzed using SRS and MALDI-MS.
- Supporting Table 3: Protein and tryptic peptide yield from the SRS platform for various biologic samples.
- Supporting Table 4: The tryptic peptides identified from SRS-bound bovine fetuin using LC-MS/MS.
- Supporting Table 5: Proteomic and glycoproteomics results for different biological samples processed using SRS.
- Supporting Table 6: N-glycans identified from DU145Ctrl and DU145KD cell lines processed and analyzed using SRS and MALDI-MS.

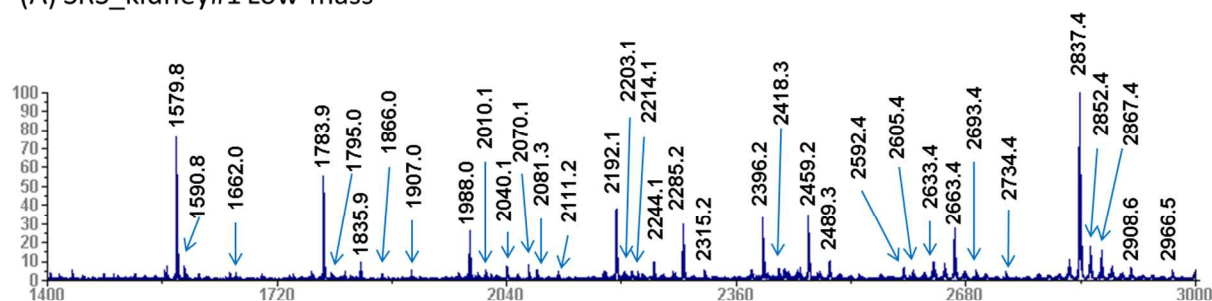


Supporting Figure 1 | Comparison of MALDI-MS spectra of permethylated N-glycans of bovine fetuin by different Sample-Prep strategies: classic solution-phase strategy **(A)**, SRS **(B)**, and SRS with fetuin dissolved in 2% SDS /PBS **(C)**. Asterisks peaks indicate that these glycans contain one or two N-glycolylneuraminic acid (Neu5Gc) residues, rather than abundant N-acetylneuraminic acid (Neu5Ac). All peaks were single sodium adducts, and the monoisotopic peaks are annotated. All peaks were assigned a putative topology based on their m/z values and N-glycosylation biosynthetic pathway. Further structural details, such as inter-residue linkage, anomericity, and branching pattern, were not determined.

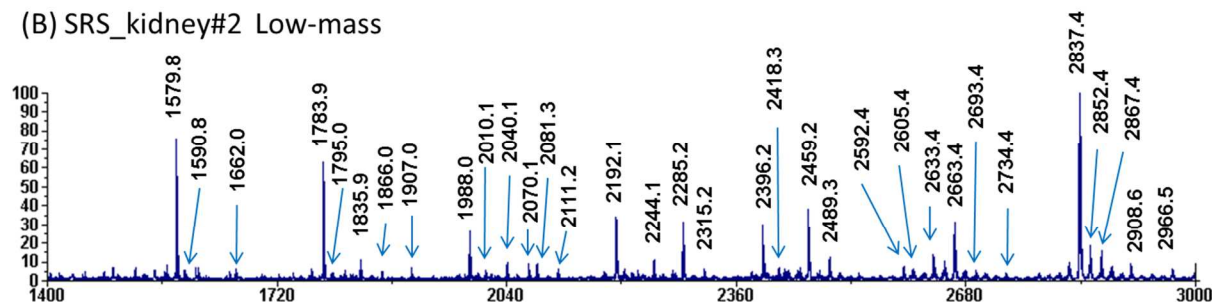


Supporting Figure 2 | Comparison of MALDI-MS spectra of N-glycans released from human serum IgG by different Sample-Prep strategies: Solution-phase **(A)**; SRS (**Replicate #1**) **(B)**; and SRS (**Replicate #2**) **(C)**. The three spectra were highly similar to each other, indicating the SRS strategy was comparable to the classical solution phase strategy. All peaks were single sodium adducts, and the monoisotopic peaks are annotated. All peaks were assigned a putative topology based on their m/z values and N-glycosylation biosynthetic pathway. Further structural details, such as inter-residue linkage, anomericity, and branching pattern, were not determined.

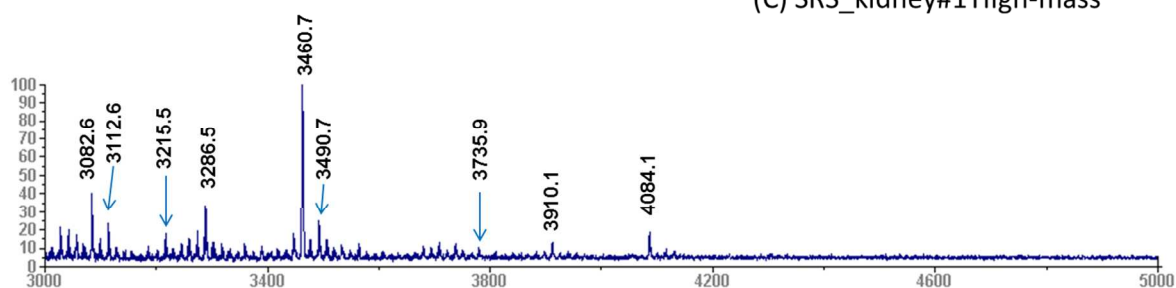
(A) SRS_kidney#1 Low-mass



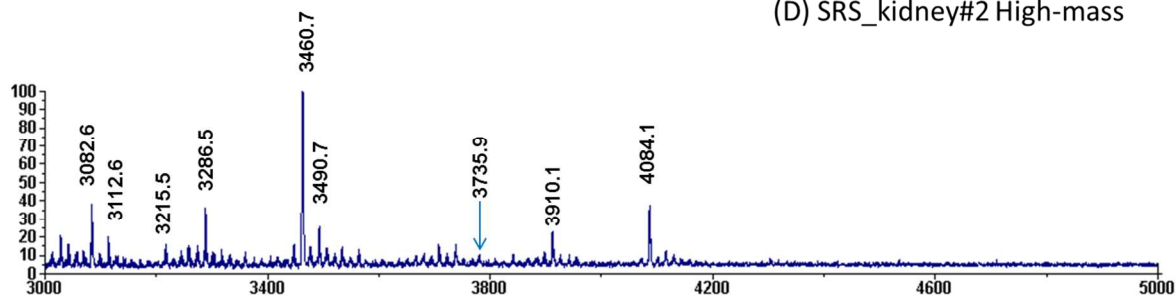
(B) SRS_kidney#2 Low-mass



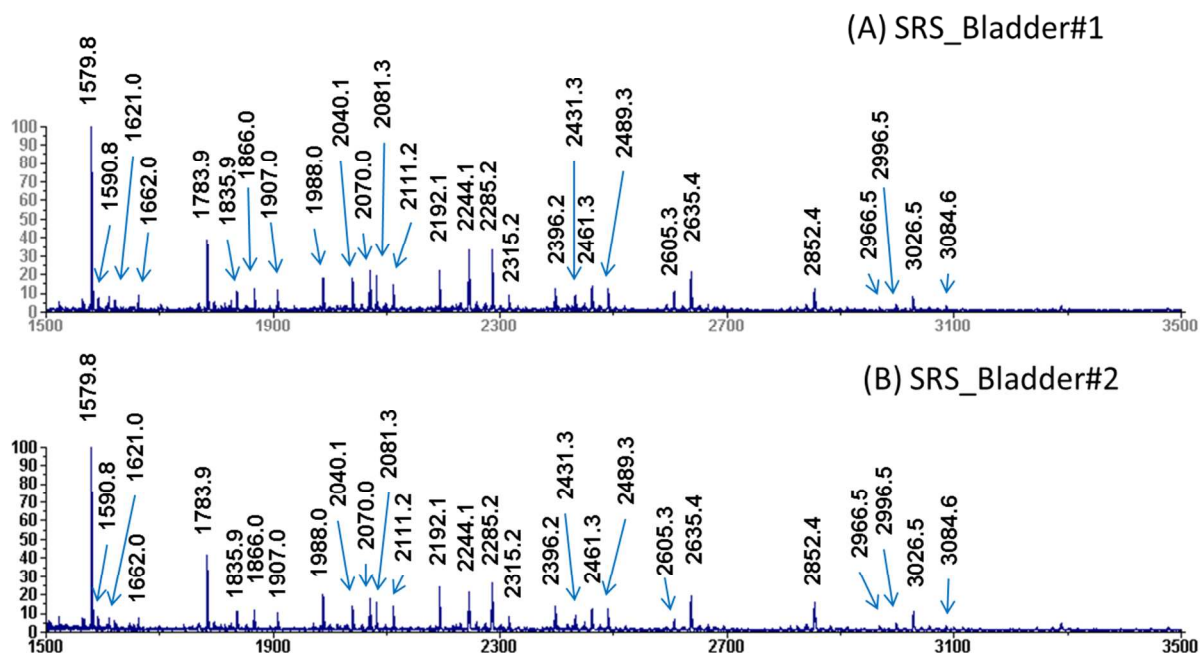
(C) SRS_kidney#1 High-mass



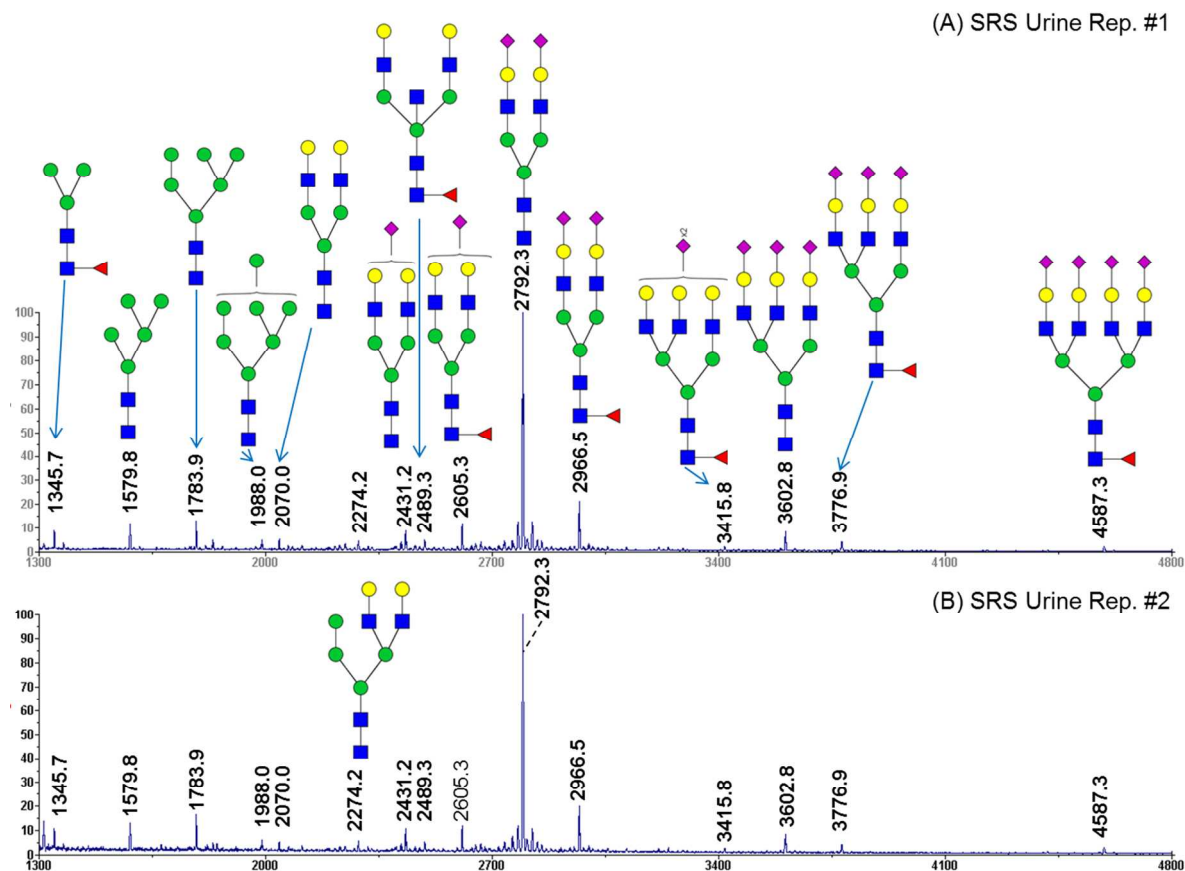
(D) SRS_kidney#2 High-mass



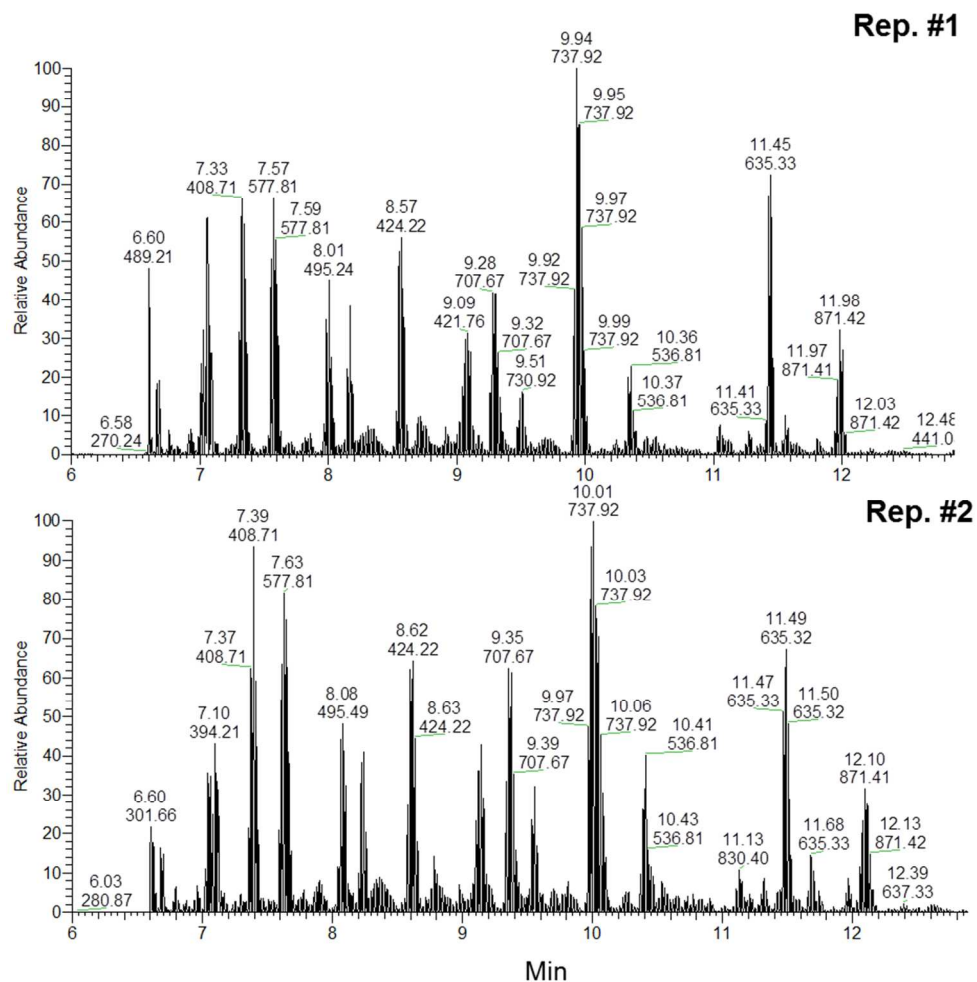
Supporting Figure 3: A comparison of the N-Glycome from two different murine kidneys (Kidney #1 vs. Kidney #2) processed and analyzed using SRS and MALDI-MS. All peaks were single sodium adducts, and the monoisotopic peaks were annotated. All peaks were assigned a putative topology based on their m/z values and N-glycosylation biosynthetic pathway as listed in **Supporting Table 1**.



Supporting Figure 4: A comparison of the N-glycome from two different murine bladder tissue samples processed and analyzed using SRS and MALDI-MS (**Bladder #1 vs. Bladder #2**). All peaks were single sodium adducts, and the monoisotopic peaks were annotated. All peaks were assigned a putative topology based on their m/z values and N-glycosylation biosynthetic pathway as listed in **Supporting Table 2**.

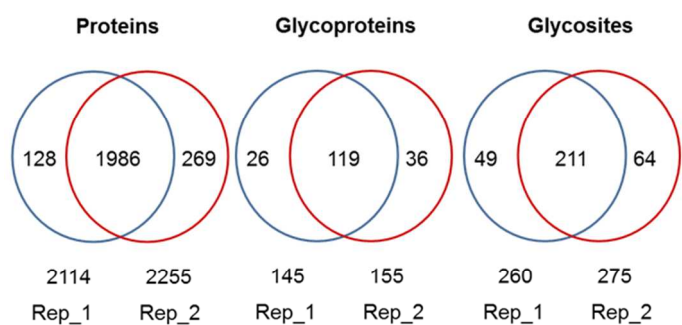


Supporting Figure 5: A comparison of a technical replicate (Rep#1, Rep#2) of the human urinary glycome obtained from a single urine sample processed and analyzed by SRS and MALDI-MS. Similar profiles were obtained for both replicates, indicating a high degree of reproducibility using the SRS approach. All peaks were single sodium adducts, and the monoisotopic peaks are annotated. The peaks were assigned a putative topology based on their m/z values and N-glycosylation biosynthetic pathway. Further structural details, such as inter-residue linkage, anomericity, and branching pattern, were not determined. [■ N-acetylglucosamine; ● mannose; ● galactose; ▲ fucose; ◆ N-acetylneuraminic acid (Neu5Ac).]

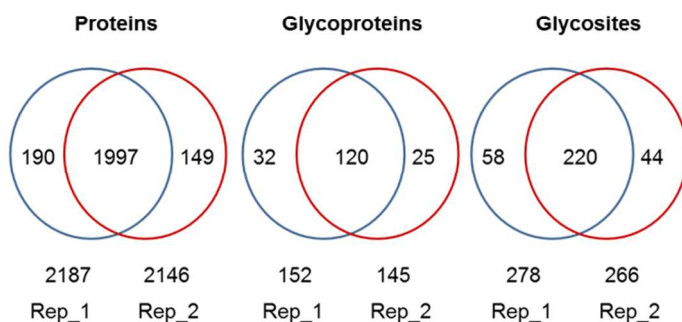


Supporting Figure 6: Replicate LC-MS/MS total ion chromatographs (TIC) of fetuin tryptic peptides obtained using the SRS strategy (**Rep #1, Rep #2**). The identified tryptic peptides are listed in **Supporting Table 5**. The TIC spectra were nearly identical between both replicates, suggesting that SRS is highly reproducible.

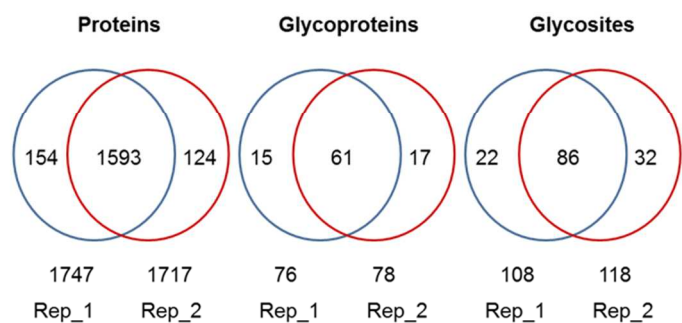
A) DU145Ctrl



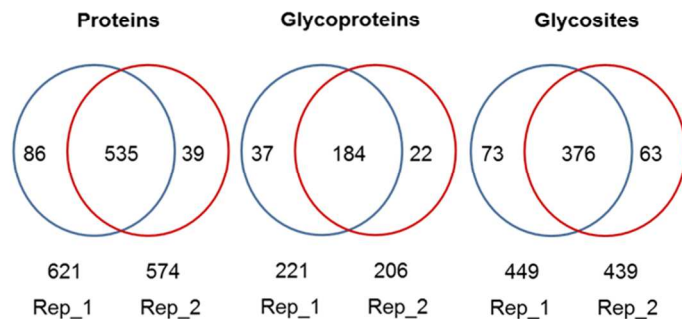
B) DU145KD



C) Mouse colon

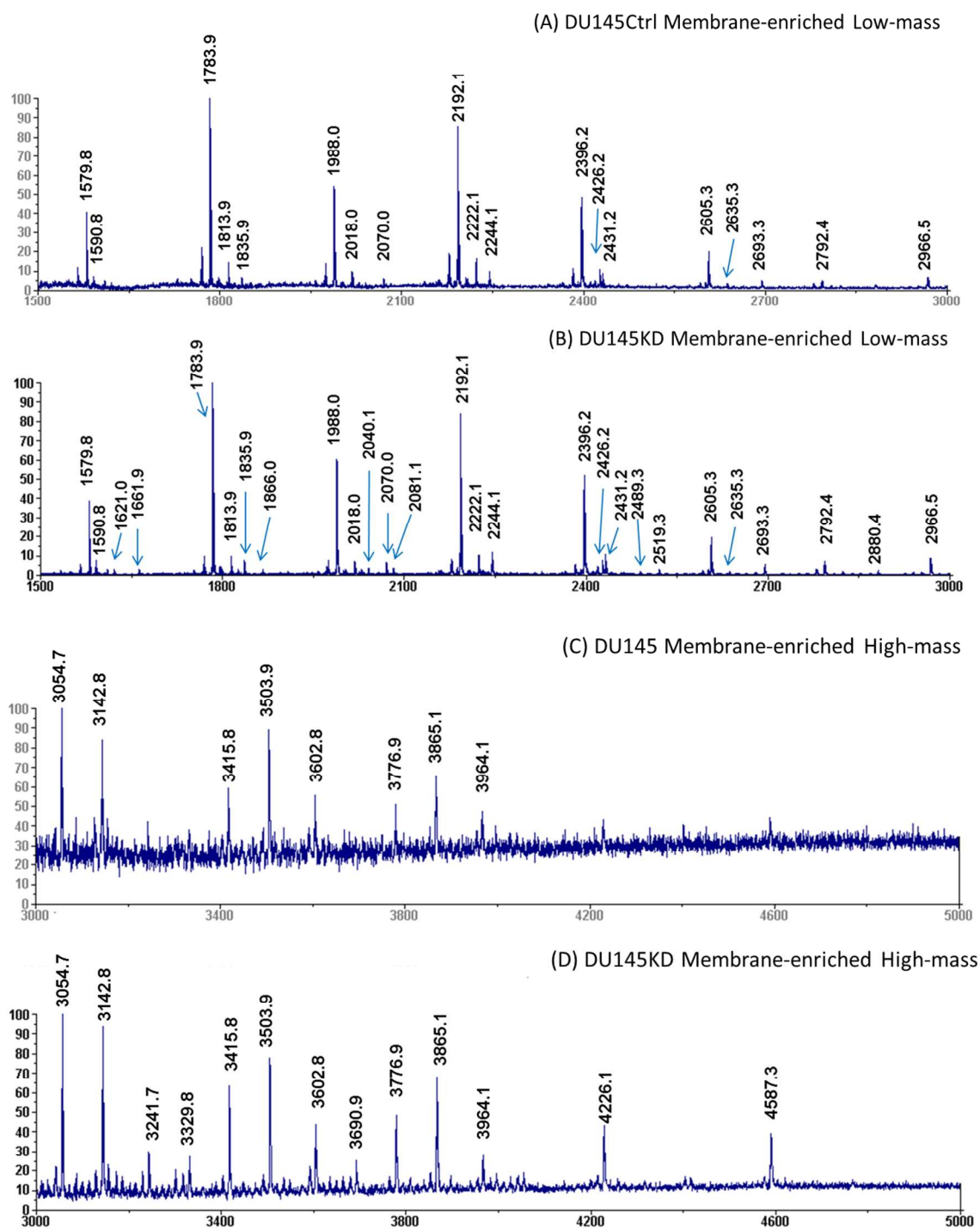


D) Adult urine specimen



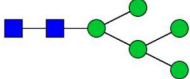
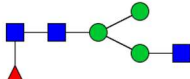
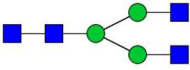
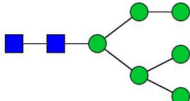
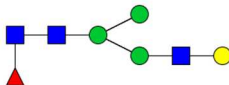
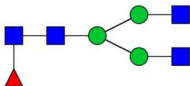
Supporting Figure 7: Proteomic and glycoproteomic comparison of technical or biologic replicates of various biologic samples processed by SRS. Venn-Diagrams represent the following: **A)** technical replicates of DU145Ctrl, membrane-enriched; **B)** technical replicates of

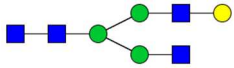
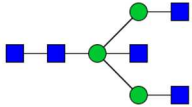
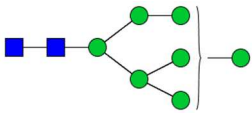
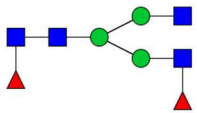
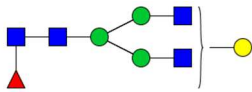
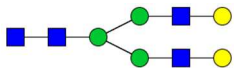
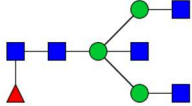
DU145KD, membrane-enriched; C) Biological replicate of murine colon; and D) technical replicate of one adult urine specimen.

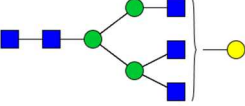
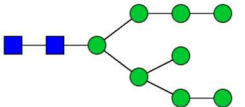
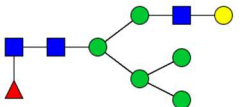
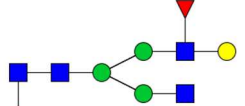
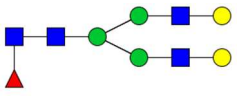
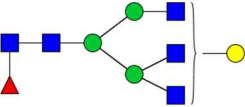
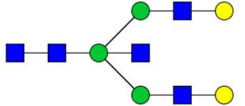


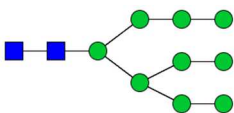
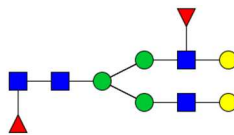
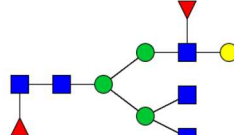
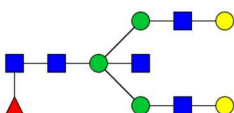
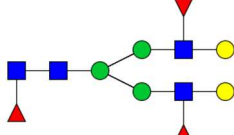
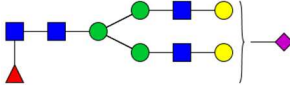
Supporting Figure 8: A comparison of the MALDI-MS spectra of permethylated N-glycans from DU145Ctrl and DU145KD cell lines obtained using SRS. All peaks were single sodium adducts, and the monoisotopic peaks were annotated. The identified peaks are listed in the **Supporting Table 7**.

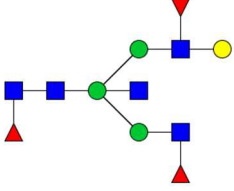
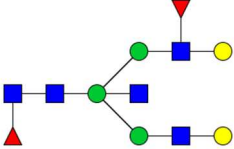
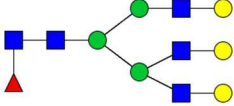
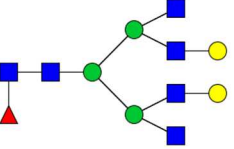
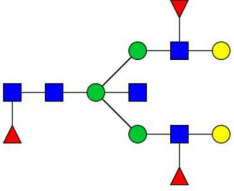
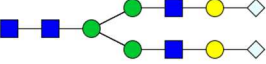
Supporting Table 1: The identified N-glycans from two different murine kidneys processed and analyzed using SRS and MALDI-MS. All peaks were assigned a putative topology based on their *m/z* values and N-glycosylation biosynthetic pathway. Further structural details, such as inter-residue linkage, anomericity, and branching pattern, were not determined. (■ N-acetyl glucosamine; ● mannose; ● galactose; ▲ fucose; ◆ N-acetylneuraminic acid (Neu5Ac); ◇ N-Glycolylneuraminic acid (Neu5Gc))

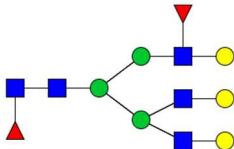
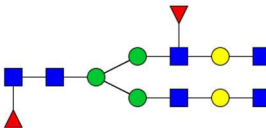
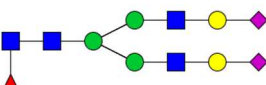
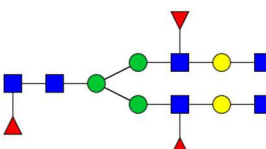
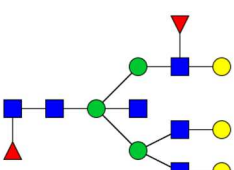
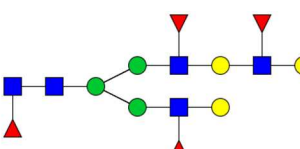
Glycan #	Observed <i>m/z</i>	Putative Topology
1	1579.8	
2	1590.8	
3	1662.0	
4	1783.9	
5	1795.0	
6	1835.9	

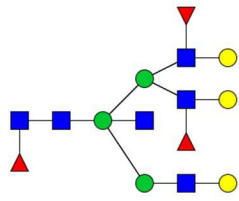
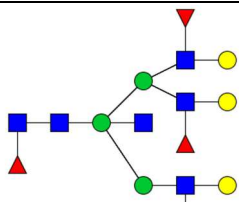
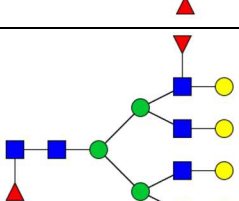
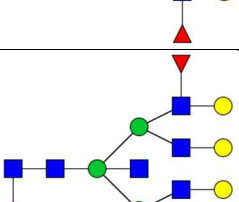
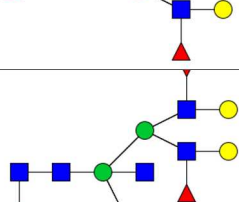
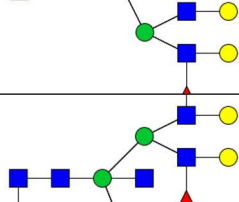
7	1866.0	
8	1907.0	
9	1988.0	
10	2010.1	
11	2040.1	
12	2070.0	
13	2081.3	

14	2111.2	
15	2192.1	
16	2203.1	
17	2214.1	
18	2244.1	
19	2285.2	
20	2315.2	

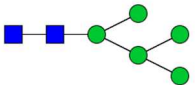
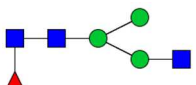
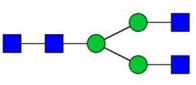
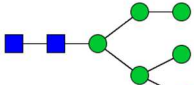
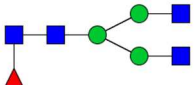
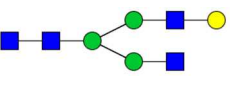
21	2396.2	
22	2418.3	
23	2459.2	
24	2489.3	
25	2592.4	
26	2605.3	

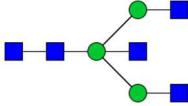
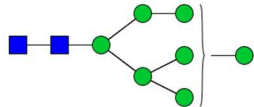
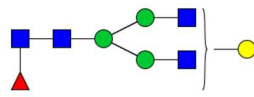
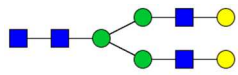
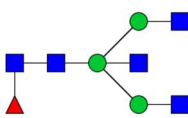
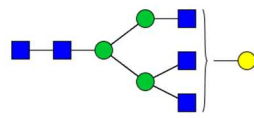
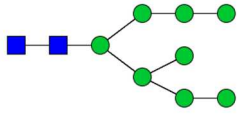
27	2633.4	
28	2663.4	
29	2693.4	
30	2734.4	
31	2837.4	
32	2852.4	

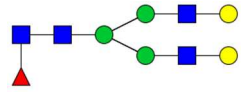
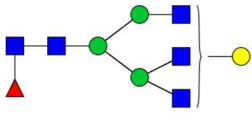
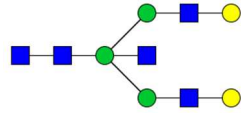
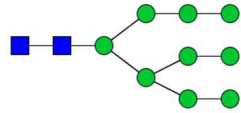
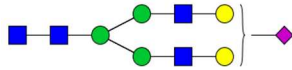
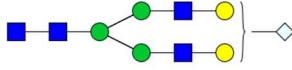
33	2867.4	
34	2908.6	
35	2966.5	
36	3082.6	
37	3112.6	
38	3215.5	

39	3286.5	
40	3460.7	
41	3490.7	
42	3735.9	
43	3910.1	
44	4084.1	

Supporting Table 2: The identified N-glycans from two different murine bladder tissue samples processed and analyzed using SRS and MALDI-MS. All peaks were assigned a putative topology based on their *m/z* values and N-glycosylation biosynthetic pathway. Further structural details, such as inter-residue linkage, anomericity, and branching pattern, were not determined. (■ N-acetyl glucosamine; ● mannose; ● galactose; ▲ fucose; ◆ N-acetylneuraminic acid (Neu5Ac); ◇ N-Glycolylneuraminic acid (Neu5Gc))

Glycan#	Observed <i>m/z</i>	Putative Topology
1	1579.8	
2	1590.8	
3	1662.0	
4	1783.9	
5	1835.9	
6	1866.0	

7	1907.0	
8	1988.0	
9	2040.1	
10	2070.0	
11	2081.3	
12	2111.2	
13	2192.1	

14	2244.1	
15	2285.2	
16	2315.2	
17	2396.2	
18	2431.3	
19	2461.3	

20	2489.3	
21	2605.3	
22	2635.4	
23	2852.4	
24	2966.5	
25	2996.5	

26	3026.5	
27	3084.6	

Supporting Table 3: Protein and tryptic peptide yield from the SRS platform for various biologic samples. Protein concentration was measured in triplicate using the BCA assay. The concentrations of peptides were estimated based on an in-house peptide concentration standard curve (A205 - Nanodrop spectrophotometer, Thermo Fisher Scientific).

Sample Types (ug)	Starting	Bound	Stripped proteins	Extracted peptides	Recovery yield (%)
Fetuin (A)	300	266	258	N/A	97
Fetuin (B)	300	289	251	N/A	87
Fetuin (C)	300	265	N/A	248	94
Fetuin (D)	300	272	N/A	251	92
Serum IgG (A)	300	282	264	N/A	94
Serum IgG (B)	300	284	272	N/A	97
Membrane-enriched DU145Ctrl (A)	400	365	N/A	321	88
Membrane-enriched DU145Ctrl (B)	400	363	N/A	315	87
Membrane-enriched DU145KD (A)	400	352	N/A	310	88
Membrane-enriched DU145KD (B)	400	359	N/A	309	86

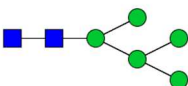
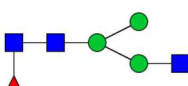
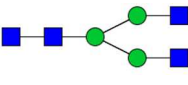
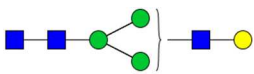
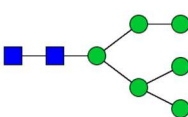
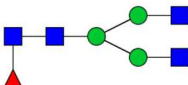
Supporting Table 4: The tryptic peptides identified from SRS-bound bovine fetuin using LC-MS/MS. The charge states of observed peptides are annotated in parentheses. Three de-N-glycosylated motifs were located within three tryptic peptides of 72-103 (NCS), 145-159 (NDS) and 160-187 (NGS). The majority of known tryptic peptides were detected, with the exception of several that were too small or too large, and not identified because of MS limitations.

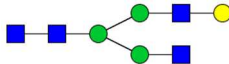
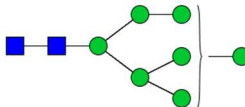
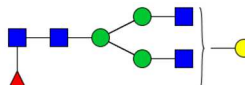
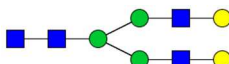
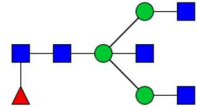
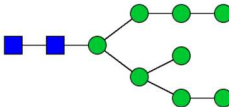
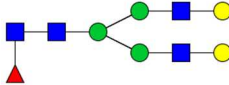
AA Positions	Peptide sequence	Calc. [M+H] ⁺	Rep.#1	Rep.#2
19-28	IPLDPVAGYK	1072.6037	536.8057 (2)	536.8055 (2)
29-50	EPACDDPDTEQAALAAVDYINK	2406.0557	1203.5417 (2)	1203.5410 (2)
51-54	HLPR	522.3152	261.6598 (2)	261.6598 (2)
55-57	GYK	367.1982	N/A	N/A
58-67	HTLNQIDSVK	1154.617	557.8101 (2)	557.8100 (2)
68-71	VWPR	557.32	N/A	N/A
72-103	RPTGEVYDIEIDTLETTCHVLDPT PLAN <u>C</u> SVR	3672.7097	1224.9082 (3)	1224.9082 (3)
104-120	QQTQHAVEGDCDIHVLK	1977.9238	659.9838 (3)	659.9812 (3)
121-131	QDGQFSVLFTK	1269.6479	635.3251 (2)	635.3242 (2)
132-143	CDSSPDSAEDVR	1337.5065	669.2568 (2)	669.2565 (2)
145-159	LCPDCPLLAPL <u>NDS</u> R	1741.7824	871.4134 (2)	871.4102 (2)
160-187	VVHAVEVALATFNAES <u>NGSL</u> QLV EISR	3017.5584	1509.2840 (2)	1509.2826 (2)
188-211	AQFVPLPVSVSVEFAVAATDCIAK	2519.3005	N/A	N/A
212-218	EVVDPTK	787.4202	394.2115 (2)	394.2140 (2)
219-225	CNLLAEK	847.4132	424.2198 (2)	424.2163 (2)
226-231	QYGFCK	802.3343	N/A	N/A
232-237	GSVIQK	631.3779	316.1905 (2)	316.1943 (2)
238-245	ALGGEDVR	816.4216	408.7124 (2)	408.7145 (2)
246-306	VTCTLFQTQPVIPQPQPDGA EAEAPSAVPDAAGPTPSAAG PPVASVVGPSVVAVPLPLHR	6015.1116	N/A	N/A
307-312	AHYDLR	774.3899	387.6964 (2)	387.6935 (2)
313-333	HTFSGVASVESSSGEAFHVGK	2120.0049	707.3426 (3)	707.3418 (3)
334-348	TPIVGQPSIPGGPVR	1474.8382	737.9231 (2)	737.9216 (2)
349-353	LCPGR	602.287	N/A	N/A
354-355	IR	288.2036	N/A	N/A
356--359	YFKI	570.3292	N/A	N/A

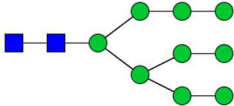
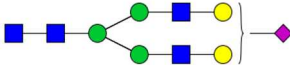
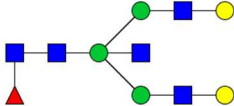
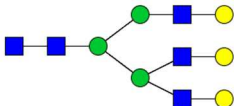
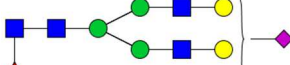
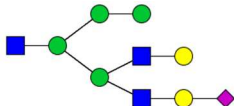
Supporting Table 5: Proteomic and glycoproteomics results for different biological samples processed using SRS. Experimental and bioinformatics procedures are described in **Experimental section**.

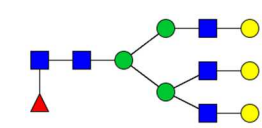
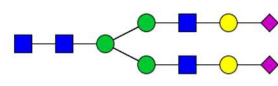
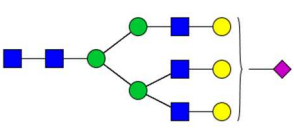
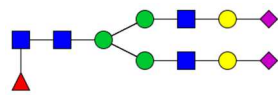
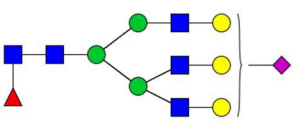
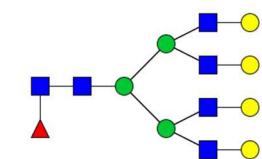
Samples	Proteins	Peptides	Deglycopeptides	Glycosites	Glycoproteins
DU145Ctrl Membrane-enriched Rep#1	2114	19699	251	260	145
DU145Ctrl Membrane-enriched Rep#2	2255	21007	270	275	155
DU145KD Membrane-enriched Rep#1	2187	19475	263	278	152
DU145KD Membrane-enriched Rep#2	2146	19010	251	264	145
DU145Ctrl Membrane-enriched Combined #1	2386	23793	319	322	179
DU145KD Membrane-enriched Combined #1	2340	21799	308	320	175
Mouse Colon Membrane-enriched Rep#1	1747	14427	106	108	76
Mouse Colon Membrane-enriched Rep b#2	1717	14152	115	118	78
Human Urine Rep#1	621	5396	455	449	221
Human Urine Rep#2	574	5218	447	439	206

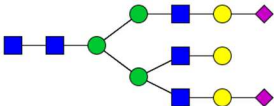
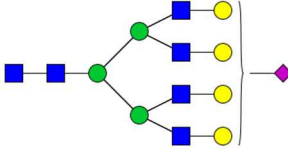
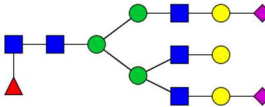
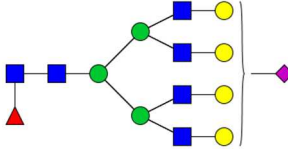
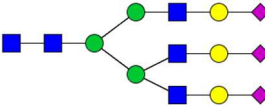
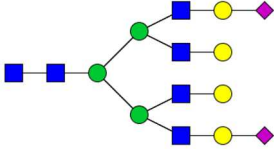
Supporting Table 6: N-glycans identified from DU145Ctrl and DU145KD cell lines processed and analyzed using SRS and MALDI-MS. All peaks were assigned a putative topology based on their *m/z* values and N-glycosylation biosynthetic pathway. Further structural details, such as inter-residue linkage, anomericity, and branching pattern, were not determined. [■ N-acetyl glucosamine; ● mannose; ● galactose; ▲ fucose; ◆ N-acetylneuraminic acid (Neu5Ac).]

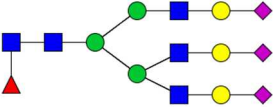
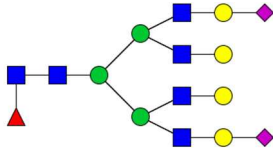
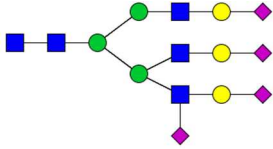
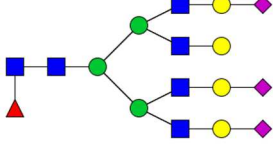
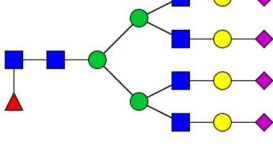
Glycan #	Observed <i>m/z</i>	Putative Glycan
1	1579.8	
2	1590.8	
3	1661.9	
4	1621.0	
5	1783.9	
6	1835.9	

7	1866.0	
8	1988.0	
9	2040.1	
10	2070.0	
11	2081.3	
12	2192.1	
13	2244.1	

14	2396.2	
15	2431.2	
16	2489.3	
17	2519.6	
18	2605.3	
19	2635.3	

20	2693.3	
21	2792.4	
22	2880.4	
23	2966.5	
24	3054.7	
25	3142.8	

26	3241.7	
27	3329.8	
28	3415.8	
29	3503.9	
30	3602.8	
31	3690.9	

32	3776.9	
33	3865.1	
34	3964.1	
35	4226.1	
36	4587.3	

1. Zhou, H., Froehlich, J.W., Briscoe, A.C. & Lee, R.S. *Mol Cell Proteomics* **12**, 2981-2991 (2013).

